ROYAL SOCIETY OPEN SCIENCE

royalsocietypublishing.org/journal/rsos

CC BY

Research

Cite this article: Gallagher T, Folkes D, Pittman M, Kaye TG, Storrs GW, Schein J. 2025 Fossilized melanosomes reveal colour patterning of a sauropod dinosaur. *R. Soc. Open Sci.* **12**: 251232.
https://doi.org/10.1098/rsos.251232

Received: 28 June 2025
Accepted: 4 November 2025

Subject Category:
Earth and environmental science

Subject Areas:
palaeontology

Keywords:
sauropod, dinosaur, fossil skin, colour patterning, melanosomes, *Diplodocus*

Author for correspondence:
Tess Gallagher
e-mails: vr22143@alumni.bristol.ac.uk; tessg233@gmail.com

Supplementary material is available online at https://doi.org/10.6084/m9.figshare.c.8164057.

THE ROYAL SOCIETY PUBLISHING

Fossilized melanosomes reveal colour patterning of a sauropod dinosaur

Tess Gallagher[1], Dan Folkes[1], Michael Pittman[2], Tom G. Kaye[3], Glen W. Storrs[4] and Jason Schein[5]

[1]Department of Palaeobiology, University of Bristol, Bristol, UK
[2]The Chinese University of Hong Kong, Hong Kong, Hong Kong
[3]Foundation for Scientific Advancement, Sierra Vista, AZ, USA
[4]Department of Geology, Cincinnati Museum of Center, Cincinnati, OH, USA
[5]Elevation Science Institute, Red Lodge, MT, USA

TG, 0009-0007-2182-7188

Integumentary fossils have improved understanding of dinosaur physiology, appearance and ecological niches. Fossil melanin and fossil melanosome organelles that produced melanin have made it possible to reconstruct dinosaur colour patterns, evidencing fundamental but previously elusive behaviours like camouflage. However, the colouration of several important groups, including sauropods, is still unknown. Here, we propose the first evidence of colouration in a sauropod based on potential melanosome-bearing epidermal scales. The fossil skin originates from juvenile diplodocids from the Mother's Day Quarry of the Morrison formation in Montana, USA. Scanning electron microscopy reveals two fossilized epidermal layers in the scales that vary in microbody and carbon density. Two distinct microbodies are grouped together and dispersed within the potential outermost epidermal layer. The first are oblong-shaped and interpreted as melanosomes. The nature of the second disc-shaped microbody is unclear, but their flat shape is reminiscent of platelet melanosomes, though they are smaller in size.

1. Introduction

Fossilized melanin and impressions of the melanosome organelles that produce this pigment have been found in a multitude of integument fossils, from feathered dinosaurs to amphibians, from the Eocene to Jurassic [1–4]. Since feathers are strictly epidermal structures, birds and other feathered dinosaurs are unable to rely on dermal cells for colouration. Dermal chromatophores are primarily responsible for colouration in

© 2025 The Authors. Published by the Royal Society under the terms of the Creative Commons Attribution License http://creativecommons.org/licenses/by/4.0/, which permits unrestricted use, provided the original author and source are credited.

Downloaded from http://royalsocietypublishing.org/rsos/article-pdf/doi/10.1098/rsos.251232/4417184/rsos.251232.pdf
by guest
on 17 December 2025

scales of non-avian reptiles and creating structural colours, while melanosomes and keratinous structures are responsible for colouration in feathers [2,3,5]. It is believed that melanosome shape diversity in feathers and hair is a direct result of the effects of high metabolism on the melanocortin system [3]. Melanosome shape diversity has been reported in multiple fossils of feathered dinosaurs, allowing for the colour patterning of these animals to be determined from the preserved melanosome impressions [2,6–8]. Only three dinosaurs with near full body scale covering have been reported to have preservation of melanin, with only one preserving melanosome impressions [9–11]. Additionally, these near full-body scaled dinosaurs have all been ornithischians. There has yet to be any evidence to suggest colour patterning in sauropods. Discoveries have shown that the structure of sauropod integument is more varied than previously thought [12–15]. The scale shapes and patterns in sauropod skin were highly variable, suggesting these animals would have had a textured and reptilian appearance in life, having potential for species-specific scale patterning akin to some hadrosaurs [16].

To begin addressing the absence of sauropod colour information, we present new observations from juvenile *Diplodocus* sp. fossils and discuss their implications for our knowledge of sauropod colour patterning and their biological significance. These fossils come from the Mother's Day Quarry, a remarkable site that is one of the few worldwide to contain juvenile sauropods and display exceptionally preserved skin [14,17,18]. The individuals at this site vary greatly in size, with the largest specimens hypothesized to be as large as modern-day megafauna. The site is Late Jurassic in age and part of the Morrison Formation, the matrix comprising siltstone and mudstone [17]. It should be noted that while one specimen from the quarry was described as *Diplodocus*, there is ongoing research on sauropod phylogenetics in the Morrison Formation that may change the classifications of these animals [19]. For this paper, the specimens are referred to as *Diplodocus*, but the classification of these animals may change with future research. The juveniles at this site are interpreted to have died during the dry season, possibly as a herd, at an ephemeral water source before water returned [17]. The bodies desiccated in the sun for weeks to months before being buried by a debris flow [17].

2. Methods

Specimens CMC VP 20857, CMC VP 20858, CMC VP 15915, CMC VP 10660 and VP 10662 were acquired and approved for destructive analysis from Cincinnati Museum Centre (CMC) based on their preservation quality, with noticeable definition of the scale shapes to the eye. A sample of sediment was taken from CMC VP 20857 to act as a control for elemental mapping. Specimen CMC VP 10659 was viewed and pictures taken under regular light microscopy and under laser-stimulated fluorescence (LSF) following the protocol used by Pittman *et al*. [15] on *Haestasaurus* based on Kaye *et al*. [20]. The other samples are hard to distinguish through images and were not viewed under LSF, so CMC VP 10659 portrays how polygonal scales typically look. Small pieces of preserved *Diplodocus* skin (CMC VP 10660, VP 10662, CMC VP 20858 and VP 15915) were chipped off using a scalpel and used for a Zeiss scanning electron microscopy (SEM). Specimen CMC VP 10660 was cut with a diamond saw to view the skin in cross section for both light microscopy and SEM. Specimens for SEM analysis were placed on pedestals with carbon tape and gold-coated before being examined. CMC VP 20858 was viewed with a Thermo Fisher Scientific Apreo S SEM and sputtered coated with platinum. Specimens were viewed both with backscatter and secondary electron imaging modes. Initially, samples were taken to be viewed under time-of-flight secondary ion mass spectrometry (TOF SIMS) to understand the secondary ions of the surface of the fossilized integument in search of melanin, as is standard for most fossil melanosome studies [9]. This proved to be ineffective at finding evidence for melanin, only showing signs of sediment on the surface of the integument. The reason for this, as discovered with SEM and elemental mapping, was due to the preservation of the fossilized epidermal layers concealing the melanosomes (see §3), hence why this study relies on SEM and elemental mapping. A spreadsheet of melanosome sizes from modern birds, non-avian reptiles and fossil taxa was provided by Jakob Vinther and organized by author D.F. and combines melanosome sizes with Li *et al*. [3] (supplements). *Diplodocus* melanosome width and length were measured by both authors T.G. and D.F. and cross-examined for human error to confirm that the sizes predicted were as accurate as possible (CMC VP 10660: $n = 32$, CMC VP 10662: $n = 16$). Melanosomes from CMC VP 15915 and CMC VP 20858 were not added to this scatter plot because they did not have a large enough sample size compared to the other specimens.

Downloaded from http://royalsocietypublishing.org/rsos/article-pdf/doi/10.1098/rsos.251232/4417184/rsos.251232.pdf
by guest
on 17 December 2025

3. Results

3.1. Scale description

The scales of CMC VP 10660, CMC VP 15915 and VP 10662 are polygonal in shape and approximately 10 mm in diameter (figure 1B,C). CMC VP 20858 consists of rounded scales approximately 1–5 mm in diameter (figure 1D). The scales in cross section under light photography appear as a flat carbonaceous film atop the sediment (figure 1A). The scales can appear as grey, black or dark brown (figure 1). CMC VP 15915 is a negative impression with small amounts of carbon in the impression (electronic supplementary material, figure S2), while CMC VP 10660 and 10 662 are positive relief carbonaceous moulds (figure 1B,C). Only CMC VP 15915 shows prominent epidermal papillae, a characteristic of sauropod scales. CMC VP 10660 and VP 10662 lacking epidermal papillae is due either to taphonomy or they were not present on these scales. It is unknown where on the body these scales originated, as polygonal scales are the most common scale type found on *Diplodocus*. The well-preserved CMC VP 106659 provides a good indication of the appearance of these polygonal scales (figure 1H,I). It is hypothesized that these scales could have originated from the dorsolateral abdomen, tail and/or limbs, based on the known placement of hexagonal and polygonal scales in *Diplodocus* from the Mother's Day Quarry [21].

3.2. Elemental mapping and clay mineral description

Cross sections of polygonal scales from CMC VP 10660 under SEM show that they consist of two layers that vary in elemental make-up (figures 2 and 3). The uppermost layer consists primarily of aluminium and silica based on EDS maps (figure 3). This top layer has a flakey texture and is composed of layered sheets (figures 2C and 3A,B). This sheeted layer can appear distorted, with the sheets appearing scrunched or rolled (figure 2A,B; electronic supplementary material, figure S3). Integument layer thickness varies greatly from approximately 5 µm, approximately 50 µm and approximately 250 µm (figures 1A and 2A,B; electronic supplementary material, figure S3). A cross-section from CMC VP 10660, which sat closer to the hinge region of the scale, is comparatively thin, only 5–10 µm thick, compared to the cross-section from the middle of the scale (electronic supplementary material, figure S3). Carbon is rare in the top layer but is most concentrated in areas which also preserve microbody impressions (figure 4). Beneath the clay mineral layer is a smooth carbon-rich layer (figures 3D,E and 4A) with many microbody impressions and moulds, some of which appear to have melded together and degraded. EDS was done on CMC VP 20858 zoomed on a cluster of disc-shaped microbodies (figure 4C; electronic supplementary material, figure S4). There was a high concentration of carbon and depleted aluminium and silica. The sediment sample from CMC VP 20857 showed an enrichment of silica and aluminium, with depleted carbon (figure 3C). The sediment can vary in appearance, sometimes exhibiting large sediment grains (<50 µm) to extremely small grains unable to be distinguished. The sediment typically exhibits a smooth granulated and random assortment under SEM as opposed to the flakey layered sheets of the skin (figures 2A,B and 3A,B; electronic supplementary material, figure S3).

The fossil skin did not appear to be rich in any elements except carbon, silica and aluminium (figures 3A,B and 4C; electronic supplementary material, figure S4). All other elements either do not conform to the shape of the skin, share a similar enrichment to the sediment or are depleted.

3.3. Microbodies description

Specimens CMC VP 10662, CMC VP 105915, CMC VP 20858 and VP 10660 possess microbody impressions (figures 1 and 2; electronic supplementary material, figures S1 and S2). Microbodies within the cross-section of CMC VP 10662 were approximately 480 nm long and approximately 237 nm wide, whereas those of CMC VP 10660 are smaller, with an average length of approximately 232 nm and width of approximately 158 nm. CMC VP 20858 microbodies average approximately 340 nm long and approximately 246 nm wide. CMC VP 10662 and VP 10660 microbodies sit within the same size range as brown melanosomes in birds (figure 5). Specimens CMC VP 10660 and VP 20858 possess two distinct microbody morphotypes, the common oblong melanosome which pairs with brown melanosomes (figure 5), as well as disc-shaped microbodies (figures 2C–E and 4). The most visible disc-shaped microbody in VP 10660 has a diameter of approximately 360 nm. Elongate, rod-like

Downloaded from http://royalsocietypublishing.org/rsos/article-pdf/doi/10.1098/rsos.251232/4417184/rsos.251232.pdf
by guest
on 17 December 2025

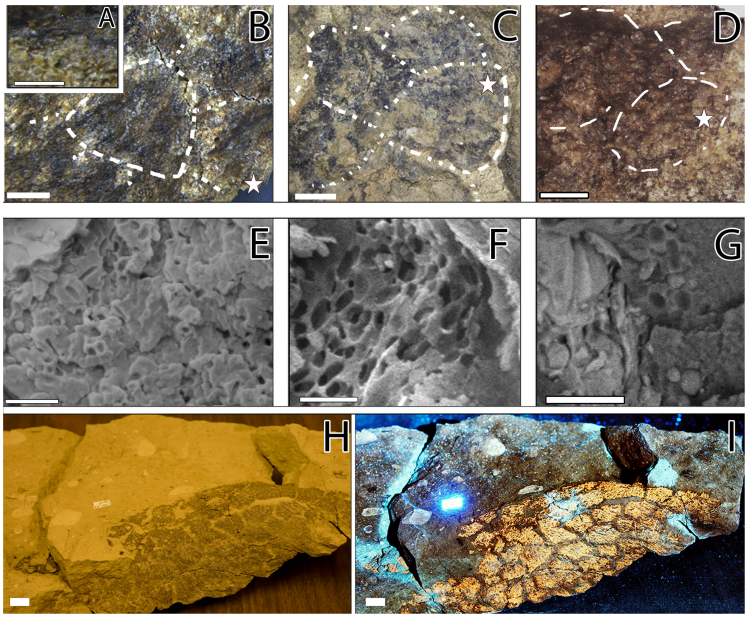

Figure 1. Sampled fossilized hexagonal scales outlined with dotted white lines, with correlated melanosome impressions and LSF image. (A) Cross-section of CMC VP 10660 showing the film of skin atop the sediment. (B) Polygonal scales from CMC VP 10660. (C) Polygonal scales from CMC VP 10662. (D) Scales from CMC VP 20858. (E–G) SEM melanosome impressions and moulds directly associated with sampled scales. Each SEM image is directly associated with the specimen pictured above it (E to A and B, F to C, and G to D). (H) Light image of the well-preserved CMC VP 10659 showing polygonal and rectangular scales. (I) CMC VP 10659 under LSF. Stars show where samples were taken from the specimens for SEM. Scale bars: 500 µm (A), 1 mm (B), 2 mm (C), 400 µm (D), 1 µm (E–G), 10 mm (H and I).

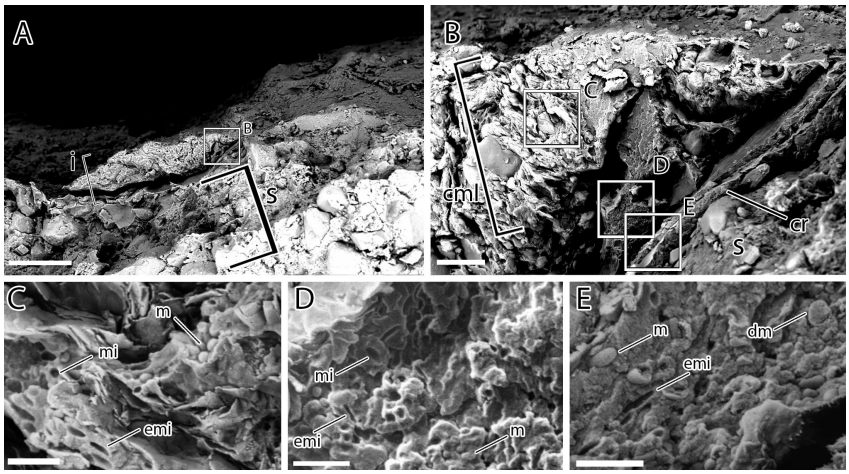

Figure 2. SEM images of a cross-section of a *Diplodocus* scale displaying melanosomes and clay mineral layering. (A) Cross-section of integument (i) on top of sediment (s). Scale bar represents 100 µm. (B) Close-up of integument showing a clear distinction in clay mineral layers (cml) overlying the carbon-rich layer (cr). Scale bar represents 10 µm. (C) Close-up of clay mineral layer displaying melanosome impressions (mi), elongate melanosome impressions (emi) and intact melanosomes (m). (D) Close-up of melanosome impressions in the partially displaced layer directly above the carbon-rich layer. (E) Close-ups of parts of the carbon-rich layer, displaying numerous melanosome impressions and elongate rod-like melanosome impressions, as well as a single disc microbody (dm). Scale bars for C–E all represent 1 µm.

impressions are also present but are most likely the result of disc-shaped microbody impressions viewed in cross-section, as there is no evidence of rod-shaped microbodies being present. CMC VP 20858 has multiple disc microbodies which average approximately 349 nm in diameter. These are also found clustered with oblong microbodies (figure 4). The microbodies from CMC VP 10660 are usually clustered together into small groups along the clay mineral layer (figures 2 and 3). The groups can sit anywhere from 10 to >100 µm apart from each other (figures 2 and 3; illustrated in figure 6). It should

Downloaded from http://royalsocietypublishing.org/rsos/article-pdf/doi/10.1098/rsos.251232/4417184/rsos.251232.pdf
by guest
on 17 December 2025

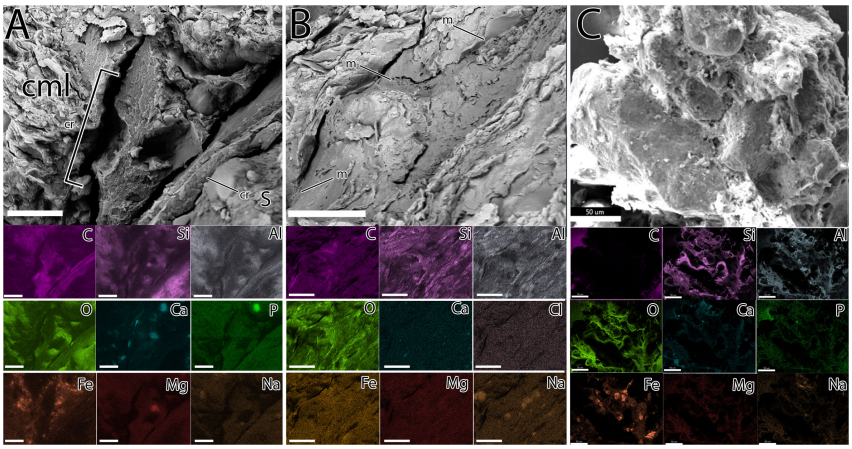

Figure 3. Elemental maps of the cross-section of CMC VP 10660 from different areas of the scale. (A) Close-up image of clay mineral layer (cml) carbon-rich melanosome layer (cr) with detached parts of the same layer showing melanosome impressions atop the sediment (S). Scale bar represents 10 µm. (B) Close-up of a clay mineral layer located farther right on the scale from A. The clay mineral layer does not possess as many melanosomes (m) as the carbon-rich layers. Note the concentration of carbon within the melanosome clusters of the clay mineral layer and carbon-rich layer. Scale bar represents 10 µm. (C) Sediment from CMC VP 20857. Scale bar represents 50 µm. Elements outlined are carbon (C), silica (Si), aluminium (Al), oxygen (O), calcium (Ca), phosphorus (P), iron (Fe), manganese (Mg) and sodium (Na).

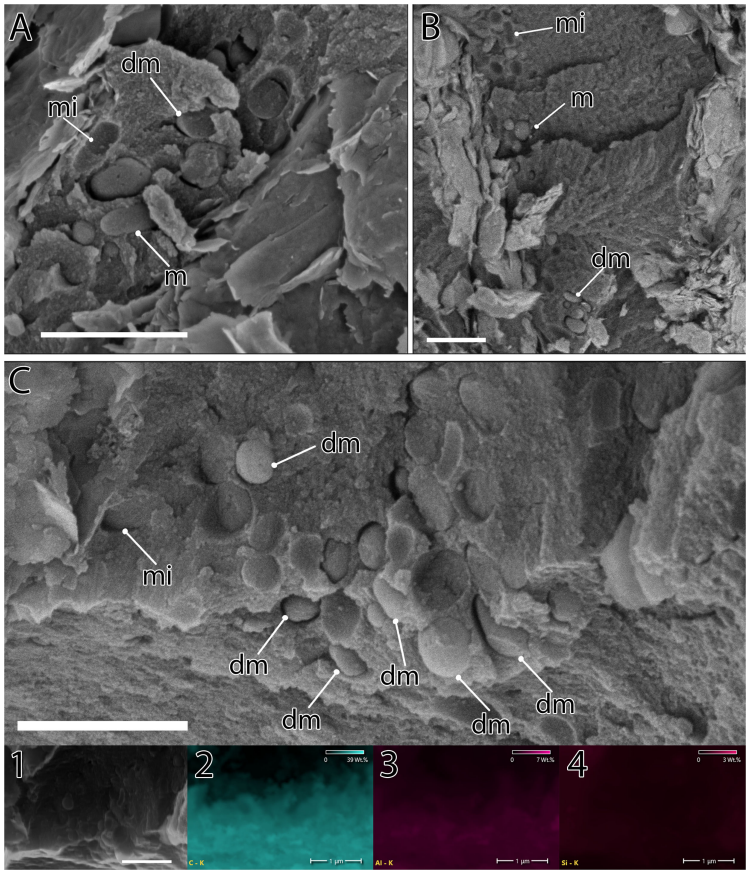

Figure 4. Microbodies of diverse morphology from a small section of stratum corneum from CMC VP 20858. (A,B) Melanosome moulds (m), melanosome impressions (mi) and disc microbodies (dm) found throughout the stratum corneum. (C) Cluster of microbodies with multiple disc microbodies (dm) poking out of the stratum corneum, with associated elemental map of the section: (1) SEM image of sampled EDS area; (2) carbon; (3) aluminium; (4) silica. Scale bars represent 1 µm.

be noted that this organization of melanosome groups, as well as the preserved aluminosilicate layer of the integument, made searching for melanosome impressions difficult. Specimen CMC VP 10662, for

Downloaded from http://royalsocietypublishing.org/rsos/article-pdf/doi/10.1098/rsos.251232/4417184/rsos.251232.pdf
by guest
on 17 December 2025

instance, only had melanosome impressions in one secluded area of the sampled integument (figure 1F; electronic supplementary material, figure S1). This was a common pattern seen among specimens that were sampled from small pieces as opposed to cross sections, such as CMC VP 15915, which only exhibited small groupings of melanosomes (electronic supplementary material, figure S2). The groups themselves can be between approximately 5 µm, approximately 20 µm and upwards of approximately 50 µm wide (figure 3A,B; illustrated in figure 6; electronic supplementary material, figures S1–S3).

4. Discussion

The Mother's Day *Diplodocus* scales represent a distinctive taphonomic scheme for integument preservation while also providing new insights into colouration and scale morphology. The presence of two distinct microbody morphotypes suggests the potential for complex colour patterning in the epidermis of juvenile *Diplodocus*.

4.1. Scale taphonomy

The oblong shape of the microbody impressions within the integument of *Diplodocus* is very similar in morphology to known fossilized melanosome impressions (figures 1 and 2). Considering the similarity in morphology and placement within the integument, the microbodies are interpreted as melanosome impressions. Feather fossils from the Jehol and Yanliao biotas are diagenetically and characteristically flattened, two-dimensional structures with only the melanosomes preserving the original feathers and calcium phosphate preserving secondarily [2,22]. However, integument fossils do not always preserve flat like the Chinese integument fossils. Specifically, epidermal scales tend to preserve as three-dimensional moulds rather than as simple two-dimensional films. Examples of this type of integument preservation include the multiple hadrosaurid 'mummies' from Cretaceous formations of North America that are famous for their three-dimensional skin preservation [16,21,23].

We hypothesize that the original keratin layer was diagenetically replaced with aluminosilicates during the fossilization process. While melanin can withstand degradation during fossilization in anoxic environments [24], keratin is not able to withstand the fossilization process. Taphonomy experiments have demonstrated that keratin will degrade and liquefy when matured at high temperatures [24,25]. In such environments, the keratin liquefies and seeps away through porous sediment, leaving behind melanosomes and, in some instances, calcium phosphate, which preserves secondarily from adenosine triphosphate (ATP) [4]. The siltstone in which the skin is preserved is highly porous, which allows easy transport of water through the matrix. The original keratin layer likely degraded away and was slowly replaced by clay minerals as water flowed through the fossil and surrounding sediment. This allowed for the melanosome impressions and moulds to remain in their original position within the upper aluminosilicate layer rather than being compressed into a flat melanosome mat, as is usually seen in feather fossils [2,6,24]. This would not be the first instance of clay minerals being reported in fossils, with examples including fossils from the Burgess Shale [26], and two hadrosaur skin samples preserved within silica and aluminium-rich sediment [10,27]. The epidermis from a specimen of the ornithischian dinosaur *Psittacosaurus* shows a similar anatomy to the *Diplodocus* specimens exhibiting a potential stratum corneum, although the epidermis in *Psittacosaurus* is primarily preserved as silica [19]. The lowermost carbon-rich layer of the skin from *Diplodocus* likely represents where melanocytes and keratinocytes would have originally been within the lowest epidermal layers of the scale, though these cells degraded and only left behind a melanin mat.

The thickness of the stratum corneum varies greatly throughout CMC VP 10660, being as thin as approximately 5 µm to as thick as approximately 250 µm (figures 1A and 2A; electronic supplementary material, figure S3). The epidermis was noticeably thin closer to the hinge region (electronic supplementary material, figure S3), but thickness varied greatly in the centre of the scale (figures 2 and 3A; illustrated in figure 6). Some of the varied thickness could be the result of the skin rolling and 'scrunching' together, likely caused by desiccation before burial. It is also possible that some of the variation in thickness, like seen between the hinge region and centre scale, could be a natural occurrence, representative of the scale epidermal thickness in life.

Downloaded from http://royalsocietypublishing.org/rsos/article-pdf/doi/10.1098/rsos.251232/4417184/rsos.251232.pdf
by guest
on 17 December 2025

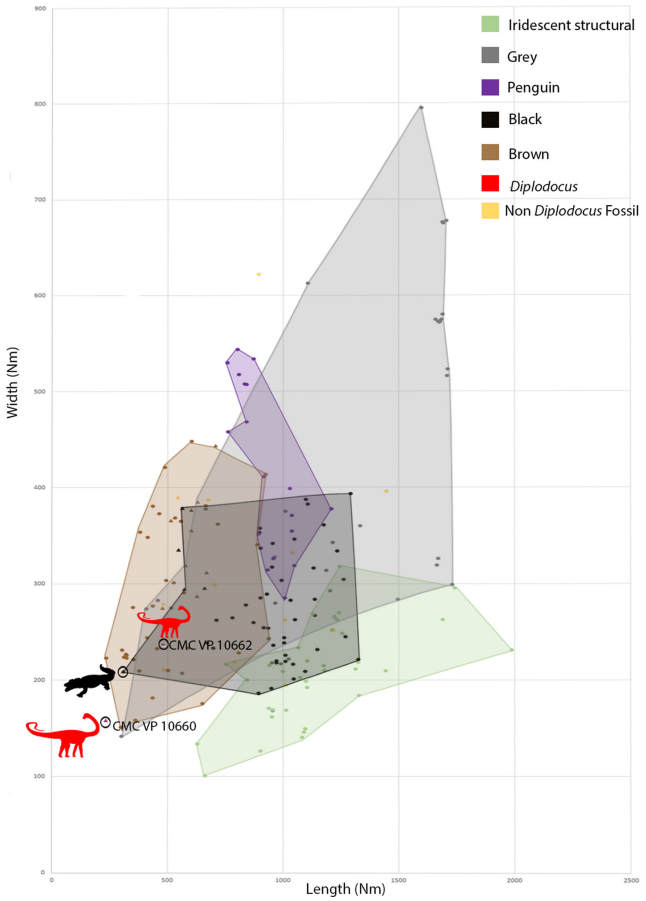

Figure 5. Scatter plot comparing *Diplodocus* melanosome size to that of modern bird (dots) and non-avian reptile melanosomes (triangles) in nanometres (nm). Penguins are placed in their own category due to their unique melanosome shapes. *Diplodocus* melanosomes represent some of the smallest melanosomes on the plot and sit closest to brown-coloured melanosomes. The closest black melanosome belongs to the black caiman, *Melanosuchus niger* (silhouetted), and is the only non-avian and non-brown melanosome that sits close to *Diplodocus*. Crocodile silhouette obtained from Phylopic.org.

4.2. Microbody positioning

It is imperative to note the difficulty in finding these melanosome impressions during our experiments as reference for future experiments on dinosaur scales. Several samples, which consisted of small pieces taken from the specimens with a scalpel, consisted only of aluminosilicate sheets and no visible melanosome impressions. Samples from CMC VP 10662 were particularly noteworthy, as they largely lacked melanosome impressions except in one area of one sample which consisted of a approximately 50 µm grouping (electronic supplementary material, figure S1). CMC VP 15915 showed a similar pattern, though these samples were smaller as the specimen had very little carbonaceous content, being a negative relief (electronic supplementary material, figure S2). It was only after viewing CMC VP 10660 through cross section that it became apparent why melanosomes were so scarce in the integument: (i) the integument preserved the fossilized stratum corneum which obscured the view of these melanosome impressions and (ii) the melanosomes were not thickly distributed throughout the scale, but rather clustered in discrete groupings, perhaps evidencing a sparse speckled patterning in the scales. The melanosome groupings in *Diplodocus* can vary in size from 5 to 50 µm (figure 2; electronic supplementary material, figures S1–S3). Within the cross section of CMC VP 10660, the visible melanosome groups in the clay mineral layer sit approximately 100 µm apart (illustrated in figure 6). The preservation of the stratum corneum proves to be both a troublesome yet incredibly important discovery in understanding the anatomy and physiology of the sauropod epidermis. The fossilized stratum corneum is also the reason surface experiments, such as TOF SIMS, were initially ineffective at finding traces of melanin. The difficulty of finding melanosomes in this study raises concerns about past dinosaur scale studies that reported a lack of melanosome impressions or melanin chemical signatures in their specimens. Future research on dinosaur scales should take into

Downloaded from http://royalsocietypublishing.org/rsos/article-pdf/doi/10.1098/rsos.251232/4417184/rsos.251232.pdf
by guest
on 17 December 2025

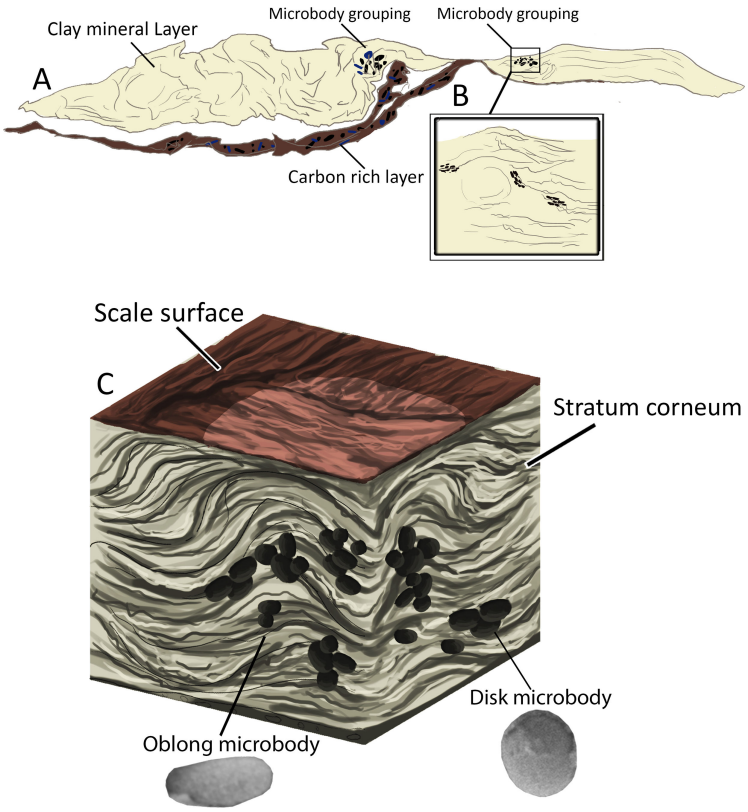

Figure 6. Interpretive reconstruction of the epidermal skin layers of the scales. Note that microbodies are not accurate to size and purely represent placement. (A) Cross-section of a portion of CMC VP 10660 distinguishing the clay mineral layer and carbon layer. (B) Melanosome group distributions based on figure 3B. (C) Interpretive reconstruction of how the stratum corneum (clay mineral layers) and melanosome placement would have looked in life based on current understanding of modern reptile integument.

consideration the possibility of their specimens being preserved similar to the ones in this study if they are to find themselves having difficulties in their methodologies.

4.3. Microbody morphologies

While modern birds show a statistically significant difference in melanosome size and colouration, there is no statistical difference between melanosome size and colouration in modern scales of non-avian reptiles [3]. The melanosomes of non-avian scale reptiles can be very small in size, akin to brown melanosomes, yet produce dark colouration as seen in *Melanosuchus niger* with average melanosome diameter of 308.6 nm length and 208.7 nm width (figure 5) [3]. Despite the *Diplodocus* microbodies plotting near brown-coloured animals in terms of size (figure 5), these microbodies may not have produced brown colouration if they are more akin to modern non-avian scale melanosomes than bird melanosomes. As *Melanosuchus* is an archosaur, this raises the question of whether the black melanosomes of *Melanosuchus* or the brown melanosomes of birds should be used to determine the pigment of *Diplodocus* melanosomes. It should be noted that maturation experiments on modern melanosomes show that melanosomes will shrink in size, so it is possible that the *Diplodocus* melanosomes would have been larger in life [28]. The lack of preserved chromatophores makes exact colouration of the integument impossible to interpret. Future analysis of the chemical composition of these melanosomes will be required to determine the exact pigment type, but this study makes a significant advance in constraining the colour of sauropods for the first time.

In CMC VP 10660, disc-shaped microbody impressions are intermixed with the oblong melanosomes in both the upper and lower layers of the skin (figure 2). The upper clay mineral layer is assumed to be the upper corneocyte layer of the epidermis (stratum corneum), which would be expected to possess only melanosomes and structural components for colour [29,30]. This is because other types of colour components such as chromatophores are living cells and thus would not be in the epidermis, which consists of dead corneocytes on the surface and living keratinocytes and

Downloaded from http://royalsocietypublishing.org/rsos/article-pdf/doi/10.1098/rsos.251232/4417184/rsos.251232.pdf
by guest
on 17 December 2025

melanocytes at the very base [29]. Numerous disc microbodies are found in CMC VP 20858 (figure 4). These structures are found in close proximity to or intermixed with oblong microbodies. The elemental mapping of the disc microbodies showed the same elemental patterns described in the other specimens, in which microbodies had a high concentration of carbon and were depleted in aluminium and silica (figure 4; electronic supplementary material, figure S4).

The closest comparisons that can be made to the disc microbodies are platelet melanosomes in modern bird feathers and the anchiornithid bird *Caihong juji*, which aid in the production of iridescent colours, as well as oblate retinal melanosomes found in the eye of an Eocene bird [2,7,31]. However, it should be noted that these disc-shaped microbodies are smaller than platelet melanosomes, the former averaging 349 nm and the latter 1000 nm [2,7,31]. It has been hypothesized that the flat, wide shape of platelet melanosomes in feathers reflects more light and can increase brightness and saturation of the feather colour [31]. The drepanosaur *Mirasaura grauvogeli* shows evidence of avian-styled melanosomes despite sitting outside of Sauria [32]. Considering the close relation between *Diplodocus* and modern birds and pterosaurs, which possess diverse melanosome morphologies [33], and the presence of avian-styled melanosome morphologies in distantly related reptiles, it is not outside the question that sauropods could have evolved complex melanosome morphologies. Considering these disc microbodies are found in the same layers as the hypothesized oblong melanosomes, are intermixed with the oblong melanosomes, share similar morphological characteristics with both modern and fossil platelet melanosomes, and show the same elemental patterns as the oblong melanosomes in the *Diplodocus* specimens, we hypothesize these disc microbodies to be melanosomes. If these disc-shaped microbodies are melanosomes, this would mark the first evidence of melanosome shape diversity within dinosaur scales and the first record among sauropods.

It is hypothesized that melanosome shape diversity in both birds and mammals is correlated to changes in the melanocortin system due to their high metabolic rates [3]. Sauropods are hypothesized to have had an endothermic metabolism akin to that of modern birds and mammals because of their gigantism and fast growth rates [34]. It is possible that, despite *Diplodocus* possessing scales, it evolved diverse melanosome shapes from the energetic effects on its melanocortin system. While the discussion of metabolism goes beyond the scope of this paper, it is interesting to note that the diversity of microbodies in the scales of juvenile *Diplodocus*, of which we hypothesize to be melanosomes, could be indirect evidence of a high metabolism in juvenile sauropods.

It can also be interpreted that the disc microbodies are a result of diagenesis, being flattened during fossilization. However, we do not support this interpretation as these structures are found next to melanosomes that show no evidence of being flattened or distorted in shape (figures 2 and 4). Additionally, melanosome moulds have been reported in full body fossilized animals that have been diagenetically flattened to a greater extent than that of the fossil skin at Mother's Day, yet the melanosomes showed no evidence of being flattened or greatly altered in shape [2,7].

Among dinosaurs, colour patterning has been described previously on the scaley skin of ornithischians. In the subadult ceratopsian *Psittacosaurus*, complex colouration featuring countershading camouflage, but also including speckling over many parts of the body, was vividly revealed under LSF [11,35]. In the adult ankylosaur *Borealopelta*, chemical detection of the melanin functional group revealed whole body camouflage and orange body colour [9]. However, neither of these dinosaurs were sufficiently preserved to show evidence of melanosomes of different shapes [9,11]. While the data in this study are limited to just four specimens of hexagonal scales, making full body colour patterning unknown, our results suggest that juvenile sauropods may have possessed diverse and unexpected melanosome morphologies.

5. Conclusions

The presence of two preserved microbody morphotypes organized within small groupings in the fossil scales of juvenile *Diplodocus* sauropods is interpreted as fossil melanosomes within preserved epidermis. The disc microbodies show that the epidermis played a more crucial role in colour production, opening the potential that sauropods produced a greater variety of colour than previously thought. Additionally, the layering of the skin suggests a different form of preservation than that of other melanin-bearing fossil integument, in which the layering of the skin may represent the original layers of the epidermis: the clay mineral layer being the stratum corneum and the carbon-rich layer being what may have once been the lower keratinocyte and melanocyte-bearing layer. This study paves the way for future work to determine the colour pattern over the entire sauropod body and provides

Downloaded from http://royalsocietypublishing.org/rsos/article-pdf/doi/10.1098/rsos.251232/4417184/rsos.251232.pdf
by guest
on 17 December 2025

the first constraints on the colour of juvenile *Diplodocus*, which are also the first constraints on the colour of sauropods in general.

Ethics. This work did not require ethical approval from a human subject or animal welfare committee.

Data accessibility. All data generated or analysed during this study are available from the corresponding author on reasonable request or included in in the published article and supplementary data [36].

Declaration of AI use. We have not used AI-assisted technologies in creating this article.

Authors' contributions. T.G.: formal analysis, investigation, methodology, writing—original draft, writing—review and editing; D.F.: formal analysis; M.P.: formal analysis, software, supervision; T.G.K.: formal analysis, software, supervision; G.W.S.: data curation, resources, validation; J.S.: resources, supervision, validation.

All authors gave final approval for publication and agreed to be held accountable for the work performed therein.

Conflict of interest declaration. We declare we have no competing interests.

Funding. The participation of M.P. and T.G.K. was supported by the General Research Fund (14116623) of the Research Grant Council (H.K.). The School of Life Sciences of the Chinese University of Hong Kong also supported M.P.

Acknowledgements. We would like to acknowledge Adel El Turke (University of Bristol) for assistance with scanning electron microscopy, Hayley Goodes (University of Bristol) for helping with diamond cutting cross-sections, Taber Yim and Craig Johnson (Drexel University) for assistance with the Thermo Fisher Scientific Apreo S SEM, Jakob Vinther (University of Bristol) for assistance in experiments and providing pre-existing melanosome size data, and Michael Chiappone (University of Minnesota) for his help with conceptualizing a dynamic colour patterning for the *Diplodocus* life reconstruction for press release. We would also like to thank Elevation Science for research guidance and collection of specimens, and the Bureau of Land Management for approval for specimen research and collection.

References

1. Colleary C *et al*. 2015 Chemical, experimental, and morphological evidence for diagenetically altered melanin in exceptionally preserved fossils. *Proc. Natl Acad. Sci. USA* **112**, 12592–12597. (doi:10.1073/pnas.1509831112)
2. Hu D *et al*. 2018 A bony-crested Jurassic dinosaur with evidence of iridescent plumage highlights complexity in early paravian evolution. *Nat. Commun*. **9**, 217. (doi:10.1038/s41467-017-02515-y)
3. Li Q, Clarke JA, Gao KQ, Zhou CF, Meng Q, Li D, D'Alba L, Shawkey MD. 2014 Melanosome evolution indicates a key physiological shift within feathered dinosaurs. *Nature* **507**, 350–353. (doi:10.1038/nature12973)
4. Roy A, Pittman M, Saitta ET, Kaye TG, Xu X. 2020 Recent advances in amniote palaeocolour reconstruction and a framework for future research. *Biol. Rev.* **95**, 22–50. (doi:10.1111/brv.12552)
5. Chen SW, Lu JY, Tung PH, Lin JH, Chiesa M, Hung BY, Yang TCK. 2021 Study of laser actions by bird's feathers with photonic crystals. *Sci. Rep*. **11**, 2430. (doi:10.1038/s41598-021-81976-0)
6. Li Q, Gao KQ, Vinther J, Shawkey MD, Clarke JA, D'Alba L, Meng Q, Briggs DEG, Prum RO. 2010 Plumage color patterns of an extinct dinosaur. *Science* **327**, 1369–1372. (doi:10.1126/science.1186290)
7. Vinther J, Briggs DEG, Prum RO, Saranathan V. 2008 The colour of fossil feathers. *Biol. Lett.* **4**, 522–525. (doi:10.1098/rsbl.2008.0302)
8. Zhang F, Kearns SL, Orr PJ, Benton MJ, Zhou Z, Johnson D, Xu X, Wang X. 2010 Fossilized melanosomes and the colour of cretaceous dinosaurs and birds. *Nature* **463**, 1075–1078. (doi:10.1038/nature08740)
9. Brown CM, Henderson DM, Vinther J, Fletcher I, Sistiaga A, Herrera J, Summons RE. 2017 An exceptionally preserved three-dimensional armored dinosaur reveals insights into coloration and cretaceous predator-prey dynamics. *Curr. Biol.* **27**, 2514–2521. (doi:10.1016/j.cub.2017.06.071)
10. Fabbri M, Wiemann J, Manucci F, Briggs DEG. 2020 Three-dimensional soft tissue preservation revealed in the skin of a non-avian dinosaur. *Palaeontology* **63**, 185–193. (doi:10.1111/pala.12470)
11. Vinther J, Nicholls R, Lautenschlager S, Pittman M, Kaye TG, Rayfield E, Mayr G, Cuthill IC. 2016 3D camouflage in an ornithischian dinosaur. *Curr. Biol*. **26**, 2456–2462. (doi:10.1016/j.cub.2016.06.065)
12. Coria RA, Chiappe LM. 2007 Embryonic skin from late Cretaceous sauropods (Dinosauria) of Auca Mahuevo, Patagonia, Argentina. *J. Paleontol*. **81**, 1528–1532. (doi:10.1666/05-150.1)
13. Czerkas SA. 1994 The history and interpretation of sauropod skin impressions. *Gaia* **10**, 173–182.
14. Gallagher T, Poole J, Schein JP. 2021 Evidence of integumentary scale diversity in the late Jurassic *Sauropod Diplodocus sp*. from the Mother's Day Quarry, Montana. *PeerJ* **9**, e11202. (doi:10.7717/peerj.11202)
15. Pittman M, Enriquez NJ, Bell PR, Kaye TG, Upchurch P. 2022 Newly detected data from *Haestasaurus* and review of sauropod skin morphology suggests early Jurassic origin of skin papillae. *Commun. Biol*. **5**, 122. (doi:10.1038/s42003-022-03062-z)
16. Bell PR. 2014 A review of hadrosaurid skin impressions. In *Hadrosaurs* (eds DA Eberth, DC Evans), pp. 572–590. Bloomington, IN: Indiana University Press.
17. Myers TS, Storrs GW. 2007 Taphonomy of the Mother's Day Quarry, Upper Jurassic Morrison Formation, south-central Montana, USA. *Palaios* **22**, 651–666. (doi:10.2110/palo.2005.p05-123r)

Downloaded from http://royalsocietypublishing.org/rsos/article-pdf/doi/10.1098/rsos.251232/4417184/rsos.251232.pdf
by guest
on 17 December 2025

18. Storrs GW, Oser SE, Aull M. 2012 Further analysis of a Late Jurassic dinosaur bone-bed from the Morrison Formation of Montana, USA, with a computed three-dimensional reconstruction. *Earth Environ. Sci. Trans. R. Soc. Edinb*. **103**, 443–458. (doi:10.1017/s1755691013000248)
19. Woodruff DC, Carr TD, Storrs GW, Waskow K, Scannella JB, Nordén KK, Wilson JP. 2018 The smallest diplodocid skull reveals cranial ontogeny and growth-related dietary changes in the largest dinosaurs. *Sci. Rep*. **8**, 14341. (doi:10.1038/s41598-018-32620-x)
20. Kaye TG, Falk AR, Pittman M, Sereno PC, Martin LD, Burnham DA, Gong E, Xu X, Wang Y. 2015 Laser-stimulated fluorescence in paleontology. *PLoS One* **10**, e0125923. (doi:10.1371/journal.pone.0125923)
21. Drumheller SK, Boyd CA, Barnes BMS, Householder ML. 2022 Biostratinomic alterations of an *Edmontosaurus* 'mummy' reveal a pathway for soft tissue preservation without invoking 'exceptional conditions'. *PLoS One* **17**, e0275240. (doi:10.1371/journal.pone.0275240)
22. Yang Z, Jiang B, Xu J, McNamara ME. 2024 Cellular structure of dinosaur scales reveals retention of reptile-type skin during the evolutionary transition to feathers. *Nat. Commun*. **15**, 4063. (doi:10.1038/s41467-024-48400-3)
23. Osborn HF. 1912 Integument of the iguanodont dinosaur *Trachodon*. *Am. Mus. Nat. Hist. Memoir.* **1**, 33.
24. Roy A, Pittman M, Kaye TG, Saitta ET. 2023 Sediment-encased pressure–temperature maturation experiments elucidate the impact of diagenesis on melanin-based fossil color and its paleobiological implications. *Paleobiology* **49**, 712–732. (doi:10.1017/pab.2023.11)
25. Saitta ET *et al*. 2017 Low fossilization potential of keratin protein revealed by experimental taphonomy. *Palaeontology* **60**, 547–556. (doi:10.1111/pala.12299)
26. Anderson EP, Schiffbauer JD, Xiao S. 2011 Taphonomic study of Ediacaran organic-walled fossils confirms the importance of clay minerals and pyrite in Burgess Shale–type preservation. *Geology* **39**, 643–646. (doi:10.1130/g31969.1)
27. Barbi M, Bell PR, Fanti F, Dynes JJ, Kolaceke A, Buttigieg J, Coulson IM, Currie PJ. 2019 Integumentary structure and composition in an exceptionally well-preserved hadrosaur (Dinosauria: Ornithischia). *PeerJ* **7**, e7875. (doi:10.7717/peerj.7875)
28. McNamara ME, Briggs DEG, Orr PJ, Field DJ, Wang Z. 2013 Experimental maturation of feathers: implications for reconstructions of fossil feather colour. *Biol. Lett*. **9**, 20130184. (doi:10.1098/rsbl.2013.0184)
29. Alibardi L. 2011 Histology, ultrastructure, and pigmentation in the horny scales of growing crocodilians. *Acta Zool*. **92**, 187–200. (doi:10.1111/j.1463-6395.2010.00469.x)
30. McNamara ME, Orr PJ, Kearns SL, Alcalá L, Anadón P, Peñalver E. 2016 Reconstructing carotenoid-based and structural coloration in fossil skin. *Curr. Biol*. **26**, 1075–1082. (doi:10.1016/j.cub.2016.02.038)
31. Nordén KK, Eliason CM, Stoddard MC. 2021 Evolution of brilliant iridescent feather nanostructures. *eLife* **10**, e71179. (doi:10.7554/eLife.71179)
32. Spiekman SNF *et al*. 2025 Triassic diapsid shows early diversification of skin appendages in reptiles. *Nature* **643**, 1297–1303. (doi:10.1038/s41586-025-09167-9)
33. Cincotta A *et al*. 2022 Pterosaur melanosomes support signalling functions for early feathers. *Nature* **604**, 684–688. (doi:10.1038/s41586-022-04622-3)
34. Sander PM *et al*. 2011 Biology of the sauropod dinosaurs: the evolution of gigantism. *Biol. Rev.* **86**, 117–155. (doi:10.1111/j.1469-185X.2010.00137.x)
35. Bell PR, Hendrickx C, Pittman M, Kaye TG, Mayr G. 2022 The exquisitely preserved integument of *Psittacosaurus* and the scaly skin of ceratopsian dinosaurs. *Commun. Biol*. **5**, 809. (doi:10.1038/s42003-022-03749-3)
36. Gallagher T, Folkes D, Pittman M, Kaye TG, Storrs DrGW, Schein J. 2025 Supplementary material from: Fossilised melanosomes reveal colour patterning of a sauropod dinosaur. FigShare (doi:10.6084/m9.figshare.c.8164057)

Downloaded from http://royalsocietypublishing.org/rsos/article-pdf/doi/10.1098/rsos.251232/4417184/rsos.251232.pdf
by guest
on 17 December 2025